DUST TRANSPORT AND ITS EFFECTS DUE TO LANDING SPACECRAFT. P. T. Metzger[1], [1]Florida Space Institute, 12354 Research Parkway, Partnership 1 Building, Suite 214, University of Central Florida, Orlando, FL 32826, philip.metzger@ucf.edu.

Introduction: Lunar lander engine exhaust blows dust, soil, gravel, and rocks at high velocity and will damage surrounding hardware such as lunar outposts, mining operations, or historic sites unless the ejecta are properly mitigated. Twenty years of research have developed a consistent picture of the physics of rocket exhaust blowing lunar soil, but significant gaps exist. No currently-available modeling method can fully predict the effects. However, the basics are understood well enough to begin designing countermeasures.

Understanding the Basic Physics: Our prior work characterized the different regimes of transport that can occur under various plume and planetary environment conditions [1-8]. While rocket exhaust can deeply crater Martian regolith, the lunar effects seen with small landers up to the 5 t (landing mass) Lunar Module are largely restricted to surface scouring a few centimeters of looser material. Lunar regolith is highly compacted deeper than a few centimeters and the lack of an atmosphere to collimate the plume prevents abrupt pressure gradients from the surface that would otherwise cause the soil to deform into a crater. However, a possible exception may occur in the permanently shadowed regions where soil may be looser (as suggested by several lines of evidence). Also, there is a major gap in our understanding about what will happen with the proposed Artemis lander (20-40 t estimated), and larger commercial landers. It is unknown whether the vastly increased thrust will be adequate to induce shearing of any sort in the highly compacted, frictional lunar soil. If it does, then the changed shape of the hole under the lander will redirect ejecta into higher ejection angles and the changed pattern of gas flow might enhance erosion or turbulent mixing of regolith with gas. Without more research, we cannot predict what will occur in these cases.

Modeling Erosion Rate: Work begun at NASA and continued at the University of Central Florida with many collaborators has developed a model of lunar landing ejecta flux for the simpler cases where only surface erosion occurs. The model was based on the available empirical data which predicts quantities of each particle size, their velocities, and impact angles for each location on the Moon, scaled by lander thrust-trajectory curve and distance to landing site [9,10]. We quantified several types of damage to neighboring hardware via analysis of the Surveyor III spacecraft that was sandblasted by the Apollo 12 landing [11] and by performing hypervelocity impacts of appropriate particle sizes and velocities onto additional materials. Based on this, Metzger wrote the relevant sections of NASA's document to protect the historic sites on the Moon. Recently, Metzger and Lane [12] used Apollo data to derive a more accurate equation of soil ejection from the lander thrust-trajectory curve. We derived a power law relation between the thrust of the vehicle and the soil erosion rate with power index 2.5, so erosion increases much faster than linearly with vehicle mass. This power index produces reasonable predictions for small landers such as ~1 t Commercial Lunar Payload Services (CLPS) landers and for the ~5 t LM, but it produces unrealistic predictions for ~40 t Artemis landers. Fig. 1 shows the erosion equation integrated over the descent profile of an Artemis lander when naïvely applying this model. It predicts a crater over 50 m deep under the lander. This is unrealistic because the model is only valid if the soil is approximately flat under the lander (shallow craters, only), and because the soil will certainly be more resistant to erosion due to its higher compaction at such depths.

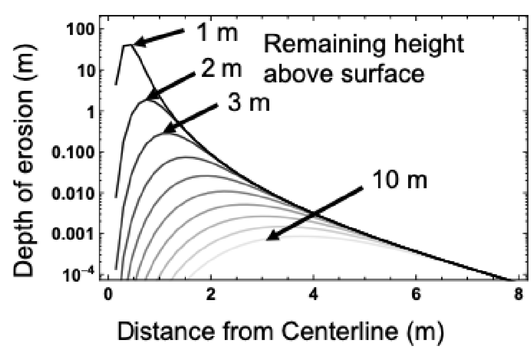

Figure 1. Prediction of naïve soil erosion model applied to a 40 t lunar lander as it descends from 10 m height down to 1 m height above the lunar surface.

This 2.5 power index also contradicts experiments in the laboratory at 1 bar ambient pressure (continuum flow regime). In those experiments the erosion rate increased linearly with thrust [13]. Other experiments in a vacuum chamber indicated that as the flow became rarefied the erosion rate began increasing faster than predicted by this unity power law [14]. We may hypothesize that the 2.5 power index observed in Apollo landings is valid in lunar vacuum while the vehicle is high so the plume on the surface is rarefied, but when the vehicle is low enough that the plume is in continuum flow then erosion rate transitions to the unity power index. Fig. 2 shows this transition for 5 t and 40 t landers.

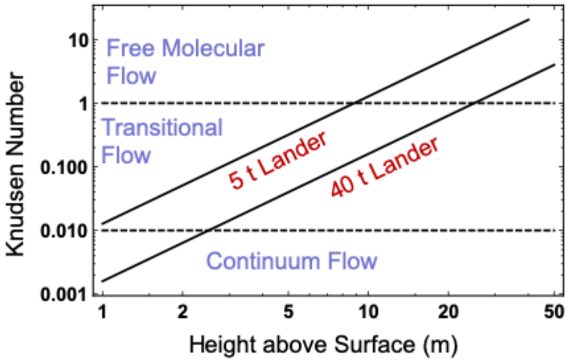

Figure 2. Knudsen number relative to radius of average lunar soil particle indicates 40 t lander will be in continuum regime for final 2.5 m of descent.

This suggests that the erosion rate may transition from 2.5 index to 1.0 index when the 40 t lander is at 2.5 m height. Per Fig. 1, the crater under the lander will be 0.5 m deep at this time, and then it will grow more slowly. If the 2.5 power index prevailed through the entire landing of the vehicle, it would eject 480 t of ejecta (compared to 2.6 t measured for the Apollo LM). If the power index transitions to 1.0 at 2.5 altitude at 2.5 m height, then a rough estimate is that the vehicle will eject a total of 108 t of regolith during its descent. This still predicts a very deep crater under the lander. On-going work is adapting the models to more quantitatively predict crater depths and ejecta masses based on this hypothesized transition of power indices. More experimental work and landings of larger lunar landers are needed to definitively solve the physics.

Trajectories of Ejecta: Analysis of LM ejecta trajectories was done by physics-based simulation [15,16] and validated as far as possible using Apollo video imagery [17,18]. The results show that the finest dust particles can be accelerated up to the exit velocity of the rocket propellant, which is 3.1 km/s for the LM's Aerozine/N_2O_4 propellants. Larger particles generally go slower with sand-size particles travelling 100-1000 m/s, gravel ~30 m/s, and fist-sized cobbles ~10 m/s. The detailed relationships are complicated because ejecta velocities depend on lander height, distance from centerline at which the particle was eroded, terrain shape, and other factors. Extrapolating to larger landers, simulations show that ejecta velocities increase logarithmically with vehicle mass, so a 40 t lander ejects material generally 50% faster than a 5 t lander. This is because the volume of the plume is larger, so the ejecta has more time to accelerate in the drag of the plume before running out into highly rarefied conditions then vacuum. Accounting for changes in propellant, the CH_4/LOX favored by SpaceX has exit velocity 3.8 km/s, and the H_2/LOX favored by NASA and Blue Origin has exit velocity 4.5 km/s. This is another factor that will increase the velocities of the ejecta. A crude estimate of maximum particle velocities as a function of size for a H_2/LOX 40 t lander is provided in Fig. 3. This is just a preliminary estimate while detailed simulations are on-going. It indicates that particles up to 10 μm can be ejected completely off the Moon.

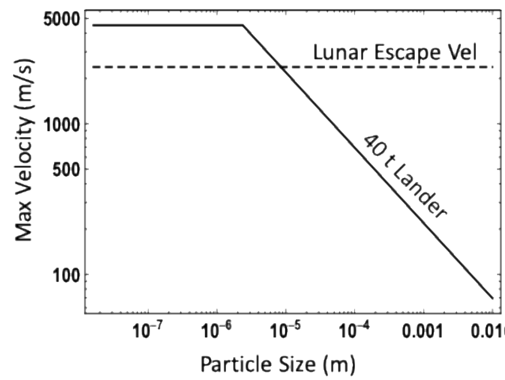

Figure 3. Model of maximum ejecta velocities as a function of lunar soil particle size.

The angles of the ejecta were also calculated by physics-based modeling and validated by Apollo imagery. Generally, the ejecta were seen travelling in a sheet close to the surface at 1 to 3 degree above the local plane. Local craters ejecta streams of dust into higher angles than this, and during the final moments of landing the plume ejects some particles from near the centerline into much higher angles, ~15 degree [16]. These simulation results were all validated by video imagery [17].

For now, global-scale modeling of ejecta trajectories has only included particles leaving the lander local in the 1-3 degree sheet. The paths of these particles travel all the way around the Moon with a significant fraction traveling higher than the Lunar Gateway orbit, as shown in Fig. 4. This ejecta sheet slowly evolves for days or weeks. Analysis is currently assessing the effects of the solar wind at possibly dispersing this ejecta sheet. Preliminary analysis indicates that the Gateway will sustain 10,000 impact/m^2 based on the 2.5 power index, or about

2,350 impact/m^2 based on the hypothesized transition to unity power index at 2.5 m altitude of the lander.

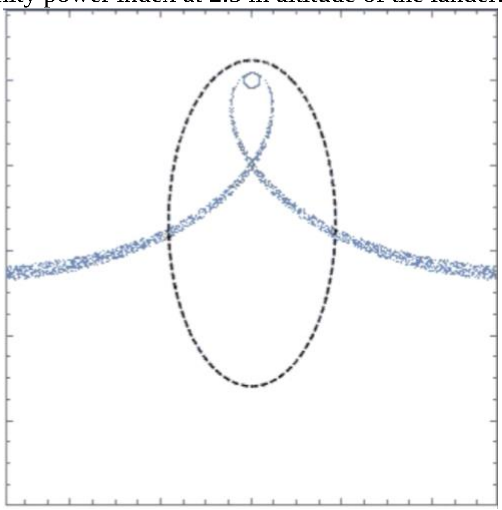

Figure 4. Cross sectional view of lunar lander ejecta (blue dots) leaving the Moon (small circle) from the landing site (top of the circle). Ejecta cross the Lunar Gateway orbit (dashed ellipse).

Impact Damage: The best information about damage from impact of these ejecta comes from the Surveyor 3 spacecraft and from experience with hypervelocity impacts in Low Earth Orbit. Surveyor 3 landed on the Moon and was visited by Apollo 12 two and a half years later. Pieces were cut off by the Apollo astronauts and brought back to Earth. The Surveyor's surface facing the Apollo LM had been sandblasted thoroughly, with more than 1 cm^2 of impacting dust per 1 cm^2 of target surface. This indicates the number of dust particles impacting it were probably at least $10^{12}/m^2$. This is much more than will impact Gateway, but they are at much lower velocity and not in the hypervelocity regime as they will be at Gateway. On Surveyor, they crushed the paint pigment and mixed dust into the paint.

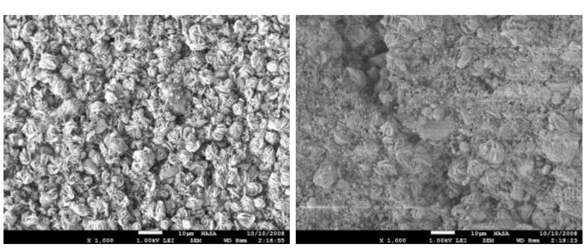

Figure 5. Scanning Electron Micrograph of Surveyor 3 paint. Left: before sandblasting by Apollo LM. Right: after sandblasting. Credit: NASA.

The Surveyor was also impacted by sand-sized particles, ~$10^6/m^2$. The sand penetrated the paint causing cracks to radiate away, so the coupon had a "dried mud cracking" appearance.

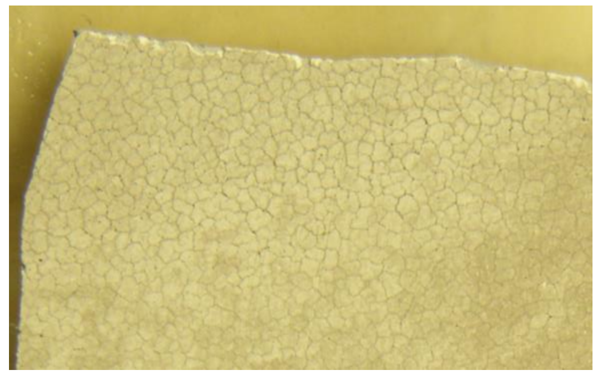

Figure 6. Mud-cracking pattern on Surveyor 3 coupon.

These are all below the hypervelocity regime. Ejecta striking orbiting spacecraft will impact at the relative velocity, which includes orbital motion. Experiments and analysis of micrometeoroid impacts in low Earth orbit show that the impactor and a portion of the taget material both vaporize. Work is on-going to quantify the amount of damage that will occur on Gateway, on spacecraft orbiting the Moon at lower altitudes, and at surface assets on the Moon as a function of distance.

Self-Damage During Landings: Not only can landers damage surrounding assets during a lunar landing, they can also damage themselves in certain conditions. If the lander is single-engine then there should be no plume recirculation so all ejecta should travel away from the vehicle. Only the landing gear should be exposed to that spray. If there is more than one engine, and if they are still firing when the lander is low enough, then the plume will recirculate between engines and this can bring ejecta back up to strike the bottom of the lander. For the case of the Surveyor 3 lander, there was no solid baseplate so ejecta was able to travel up, through the structure, and impact equipment attached to the lander's frame. The lander had an off-nominal landing because the three Vernier engines were not shut off quickly enough so the spacecraft bounced twice before final landing. After landing, the camera provided degraded imagery and this was attributed to dust deposited on the camera during the off-nominal landing. After the camera was returned to Earth by the Apollo 12 astronauts, it was found to have two "shadowlines" drawn across its mirror as shown in Fig. 7. Nickle [19] described these lines as either adhered dust or small pits caused by impacting dust, and that the shadow lines were an abrupt change in their density.

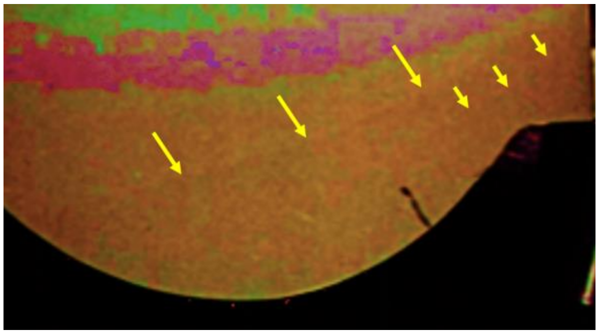

Figure 7. Shadow lines (annotated by yellow arrows) on the Surveyor 3 camera. Detail enhanced from [19].

Nickle [19] analyzed the pointing direction of the camera through the mission and possible locations on the surface from which dust must have been ejected to cause these two lines. He found that the were either caused during landing or toward the end of the mission as the Surveyor scoop was dropping soil on the surface for geotechnical testing. Because the drop test locations coincided with the possible sites for etching exactly these curves, he concluded that was the most likely explanation. Here, an argument is presented that the shadow lines were actually plume damage. First, the lines are too sharp to have been caused by low-velocity ejecta. Second, analysis of the kinetics shows that low-velocity granular splashes would not be capable of reaching the camera from that distance. Third, there were far more than two drop tests so there should have been far more than two shadow lines, but the two bounces during landing neatly explains the two shadow lines if pluming is the explanation. Fourth, the quantity of splashed material on the mirror extended over 2 pi radians would be excessive for a singular splash event, so this quantity must be from a continuous flow, not a splash. Fifth, the point sources analyzed by Nickle did not (apparently) provide perfect fits to the shadow ines. If they were from pluming, they would not be point sources but from lines sources along the plume reflection planes. It is possible, although beyond the present scope to prove, that the exact shape may be fit by line sources. Plume reflection planes are not fixed in location, but move according to relative thrust of the engines. Because the Surveyor was bouncing on the sloped inner surface of a crater and was trying to maintain level flight, the engines would have been throttled differently from each other. Fig. 8 shows the locations of the plume reflection planes for one hypothetical case of throttled engines.

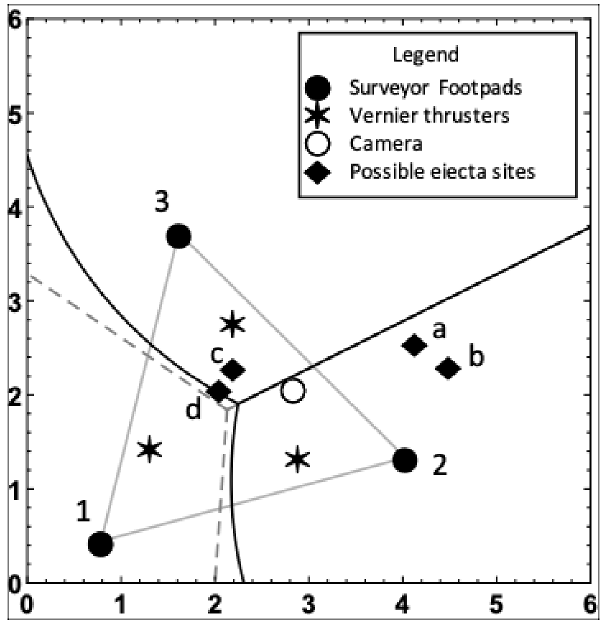

Figure 8. Location of the two pairs of possible ejecta sites per analysis of Nickle [17], showing one pair (a, b) coinciding with robotic arm soil splash tests, and another pair (c, d) coinciding closely with plume reflection planes under the lander. Dashed lines: ejecta planes with equal thrust. Solid lines: one possible case with unequal thrusts. The camera was pointed toward Footpad 3 during landing.

The re-analysis indicates the shadow lines were caused by direct sandblasting of the Surveyor's own engines during landing during the two bounces where the engines were still firing close to the surface, setting up strong fountain flow along the plume reflection planes. This also suggests the tan color noted all over the Surveyor might be caused by deposition from the off-nominal landing. The mineral of adhered dust on the east and west sides of Surveyor were found to be different [20]. This may be due to the additional sandblasting on only one side of Surveyor due to Apollo 12 landing, or some other mechanism at work.

Shock Splash During Engine Shutdown: Another mystery has been what caused the photometric disturbances to the lunar surface around each lunar landing [21,22]. These disturbances are roughly 75 m radius from the LM. The high velocities of the ejecta do not predict abrupt discontinuities in surface effects at such short distance, or any distance. Another mystery is the observed dust clearing that takes place in the field of view out the LM windows for approximately 20 s after engine shutdown [18,20]. A new model was written, assuming dust can bounce when they fall upon a much larger particle, in hopes to explain how dust stayed aloft for 20 s after engine cutoff. The fraction of each particle size that can bounce is shown in Fig. 9.

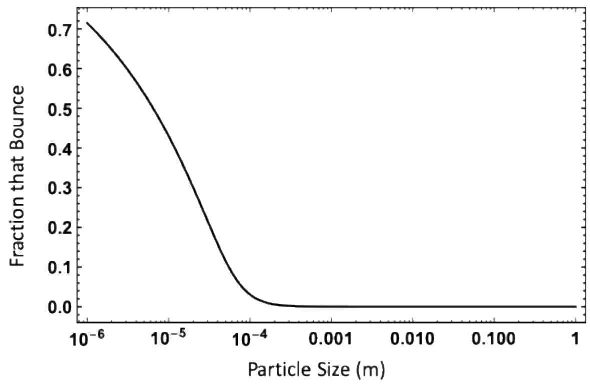

Figure 9. Fraction of each particle size that will bounce by randomly falling on a larger particle.

The mode showed that even with bouncing the dust should clear the view within just a fraction of a second and will spread over thousands of kilometers before it stops bouncing. The only way to reproduce the clearing time is to assume the dust start from a much lower initial velocity than plume ejection will cause. When we assume the particles start with only 3% of the velocities they would have from standard plume ejection, the model predicts accurately both the radius of the photometric disturbance and the dust clearing curve with correct timing. In at least one of the Apollo landing videos, we see the haziness in the field of view begins as soon as the engine is shut off, and in at least one video we see the field of view clears closer to the LM first, and then the clarity moves radially outward. All these clues suggest a common explanation: these are the result of a splash event that occurs when the engine is shut off. It is known that shutting off a supersonic rocket engine causes shockwave collapse to slap the surface under the engine [23]. The model of initial velocities derived from Apollo landings [10] was curve fitted onto results from physics-based simulations of particles of different sizes, and the resulting equation evaluated at LM height of 1.3 m is $v=2.01\ D^{-0.5}$ where v is in km/s and D is in m. For a splash the distribution of velocities may have a different shape, so we try $v=(3\%)(2.01)\ D^{-b}$ where b is an empirical parameter between 0 and 1. The resulting radius of the splash zone is shown in Fig. 10. The zone has the correct (approximate) radius of 75 m, but its edge is more or less sharp depending on the initial velocity function. This is a testable prediction. The model also predicts the correct ~20 s decay in optical density as seen out the LM window, but the curves are somewhat different with choices of b. Overall, it seems likely the engine shutting off causes a splash that drapes dust over ~75 m radius around the landing site.

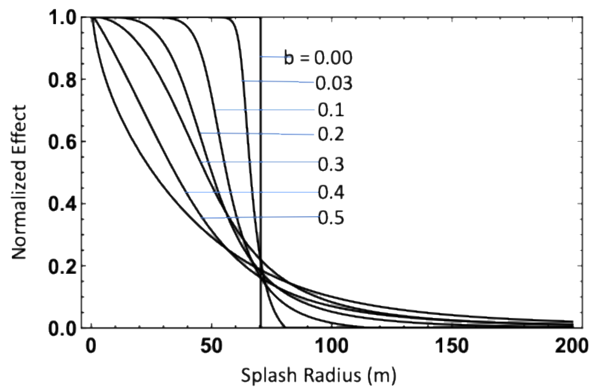

Figure 10. Normalized effect, showing how photometric disturbance might taper off with distance depending on initial velocity function.

Acknowledgments: This work was funded by NASA grant number 80NSSC19K1202.

References: [1] Metzger PT et al. (2009), Powders & Grains. [2] Metzger PT et al. (2009) AIAA 2009-1204. [3] Metzger PT et al. (2009) *J. Aerosp. Engr.*22(1), 24-32. [4] Metzger PT et al. (2011) *JGR-Planets* 116, E06005. [5] Mehta M et al. (2011) *Icarus* 211(1), 172-194. [6] Shipley ST, Metzger PT, Lane JE (2014) Earth and Space 2014. [7] Morris AB et al. (2015) *J Spacecraft & Rockets* 52(2), 362-374. [8] Morris AB et al. (2015) *AIAA J* 54(4), 1339-49. [9] Immer CD et al. (2011) *Icarus* 214, 46–52. [10] Lane JE, Metzger PT (2012) *Partic Sci & Tech* 30(2), 196-208. [11] Immer CD et al. (2011) *Icarus* 211(2), 1089-1102. [12] Lane JE, Metzger PT (2014) *Acta Geophys* 63 (2), 568-599. [13] Metzger PT et al. (2010) Earth and Space 2010. [14] Metzger PT (2016) Earth and Space 2016. [15] Lane JE et al. (2010) Earth and Space 2010. [16] Lane, JE and Metzger PT (2012) *Particul Sci and Tech* 30(2), 196-208. [17] Immer CD et al. (2011) *Icarus* 214, 46–52. [18] Metzger PT et al. (2011) *JGR Planets* 116, E06005. [19] Nickle NL (1972) Part D. In: *Analysis of Surveyor 3 material and photographs returned by Apollo 12*, NASA, pp. 51-59. [20] Lane JE (2012) *Earth and Space 2012*. [21] Clegg RN et al. (2014) *Icarus* 227, 176-194. [22] Clegg-Watkins RN (2016) *Icarus* 273, 84-95. [23] Mehta M et al. (2007) *43rd AIAA/ASME/SAE/ASEE Joint Propulsion Conf & Exhib*, 5707.